B.A.N. 17, no. 7, 511–519

Communication from the Observatory at Leiden and the Netherlands Foundation for Radio Astronomy

A HIGH VELOCITY HYDROGEN CLOUD AT LOW GALACTIC LATITUDE

STEPHEN W. PRATA*

Received July 17, 1964

Twenty-one centimeter observations reveal the existence of a high velocity feature near $l^{II} = 22°$, $b^{II} = -4°$; the feature is approximately 3° in diameter and has a mean velocity of + 115.8 km/sec and a velocity dispersion of 8.6 km/sec. Several alternative interpretations of the observations are discussed in terms of the dynamical properties of a proposed hydrogen cloud.

1. Observations

In a preliminary survey of a 21-cm study currently being made by W. W. Shane, G. P. Smith (now Mrs. Bieger) noted a few distinctive features possessing abnormally high radial velocities and seemingly separate from the ordinary galactic structure. Mrs. Bieger-Smith has discussed one of these features located at $l^{II} = 40°.5$, $b^{II} = -15°.0$ (SMITH, 1963). The present paper presents and discusses new observations which Shane programmed for the feature at $l^{II} = 22°, b^{II} = -4°$.

The observations were made with the eight-channel parametric receiver at Dwingeloo. The half-power beamwidth is 0°. 56, and an equivalent bandwidth of 20 kc/s or 4.2 km/sec was used. C. A. Muller will discuss the receiver in detail in a forthcoming article. The data were reduced on the Leiden University computing center's Electrologica X1 electronic computer, using the reduction programme written by Raimond, Hoekema and Hirsch (RAIMOND, 1962/63). Velocities are given with respect to the local standard of rest. The

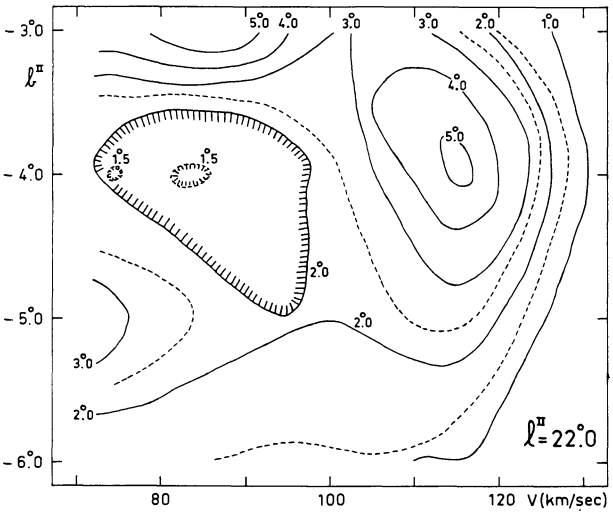

Figure 1a. Contour maps of brightness temperature as a function of velocity and one galactic coordinate; in figure 1a of galactic latitude b^{II}, at longitude $l^{II} = 22°.0$; in figure 1b of galactic longitude l^{II}, at latitude $b^{II} = -4°.0$.

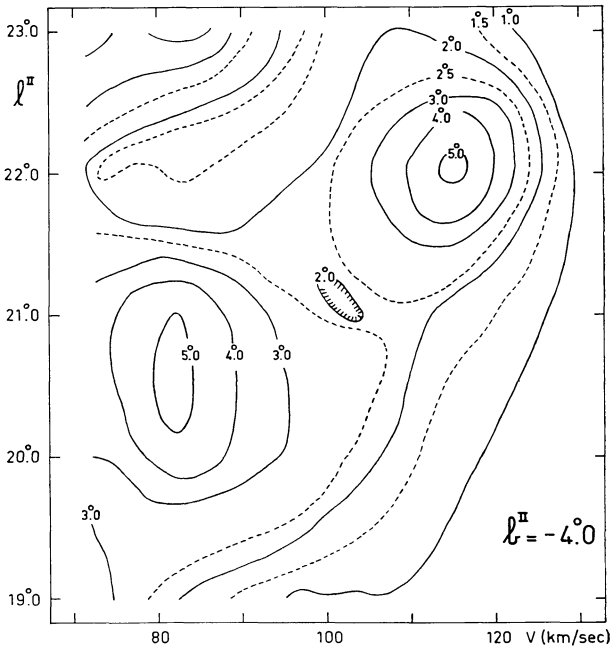

Figure 1b.

* Present address: Leuschner Observatory, Campbell Hall, University of California, Berkeley, 4, Calif., U.S.A.

observations are in two overlapping 1° grids, one covering the region bounded by $l^{II} = 19°.0$, $l^{II} = 23°.0$, $b^{II} = -3°.0$, $b^{II} = -6°.0$; and one covering the region bounded by $l^{II} = 19°.5$, $l^{II} = 22°.5$, $b^{II} = -3°.5$, $b^{II} = -5°.5$. The research was supported by the Netherlands Organization for the Advancement of Pure Research (Z.W.O.). The new observations verify the presence of the feature. Figures 1a and 1b present contour maps of brightness temperature as a function of velocity and galactic latitude and as a function of

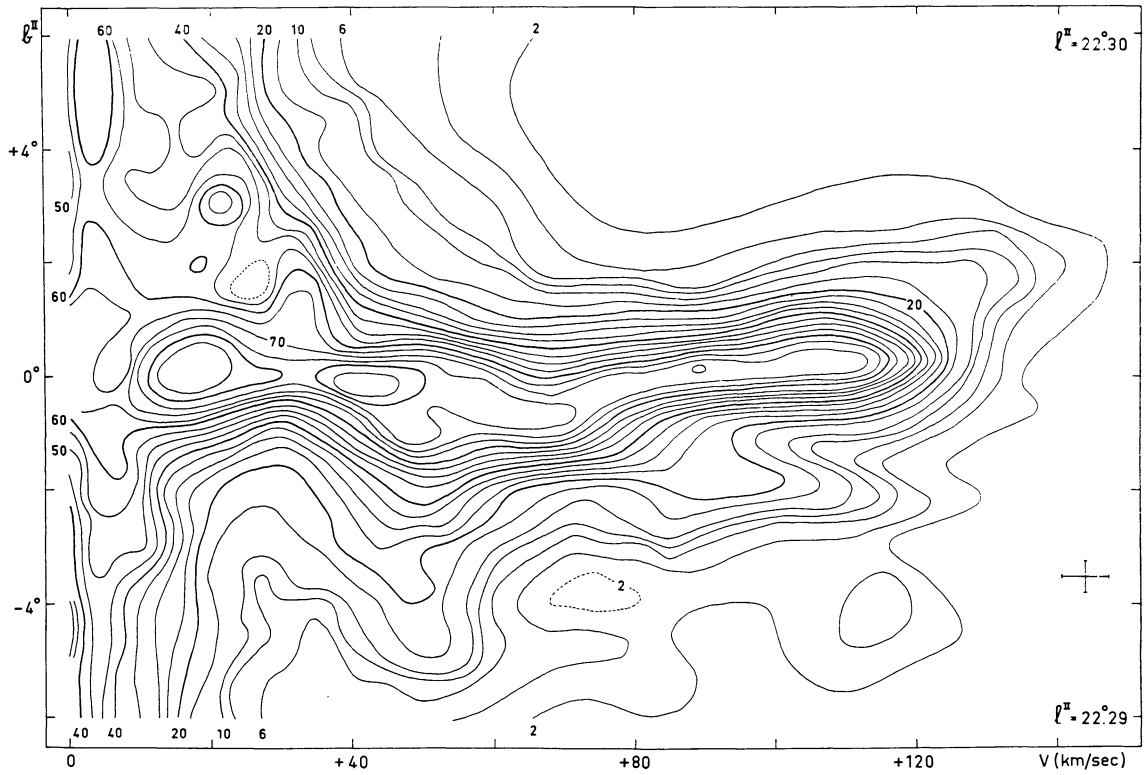

Figure 2. Contour map of brightness temperature as a function of velocity and galactic latitude at longitude $l^{II} = 22°.3$.

velocity and galactic longitude, respectively. Figure 1a is a cross section at $l^{II} = 22°.0$, and figure 1b is at $b^{II} = -4°.0$. The feature appears in both as closed contours around $V = 116$ km/sec. The closed contours in figure 1b near $V = 84$ km/sec represent an extension down from the galactic plane; thus there are no closed contours near $V = 84$ km/sec on the constant longitude map. The feature may represent a more extreme development of such a tongue. Figure 2 is a smaller scale contour map from Shane's study; the feature discussed here is in the lower right-hand quadrant. Figure 3a contains three typical line profiles. To varying degrees the lower velocity portions of the observations are complicated by radiation from the ordinary galactic structure. This effect can be noted also in figures 4a, b, and c, which give intensity contours at constant frequencies. The superposition of radiation necessitated an attempt to subtract extrapolated intensities of the ordinary galactic structure from the observations in order to obtain a clearer picture of the feature. The general procedure used was to consider two profiles at nearby points in the sky, one in which the feature was strong, the other in which it was weak. The weaker profile was then smoothed out in the vicinity of 116 km/sec to reduce residual traces of the cloud. The smoothed out profile was then scaled to match the other profile at $V = 80.4$ km/sec. In some cases the comparison profile was shifted 2.1 km/sec to bring the peaks near $V = 84$ km/sec into coincidence. This comparison profile, representing an approximation to the galactic

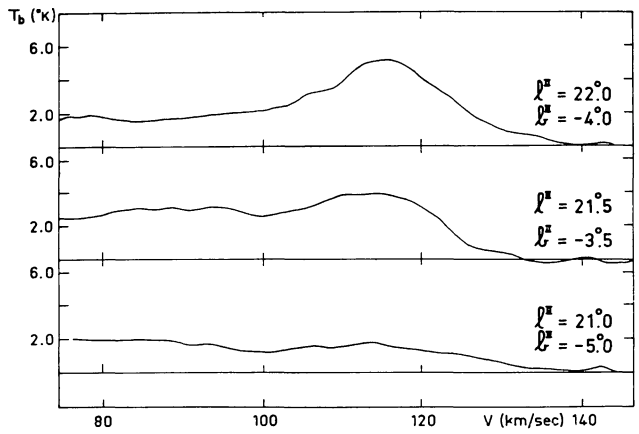

Figure 3a.

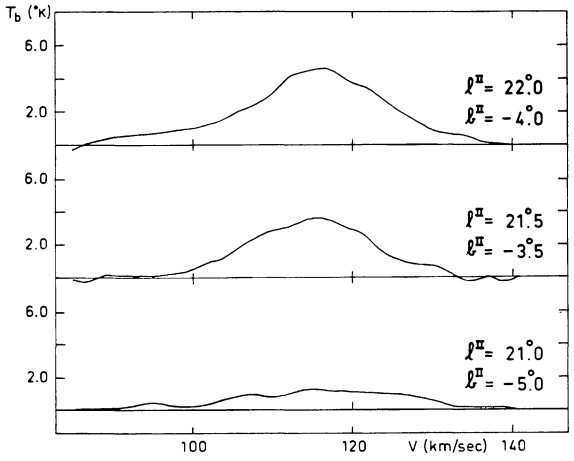

Figure 3b.

Three representative line profiles showing the feature as observed (figure 3a) and after subtraction of the extrapolated contribution of the normal galactic structure (figure 3b).

structure proper, was subtracted from the profile in which the feature was stronger. The resulting profile was then taken to represent the feature. It should be noted that the smoothing out process precludes any allowance for pecularities of the normal galactic structure in the immediate frequency range of the feature.

Figure 3b shows the profiles obtained from figure 3a by the above process. Figure 4d gives the intensity contour map for $V = 109.7$ km/sec as derived from the altered profiles. Its general shape agrees with figure 4c, where the galactic influence is small, and with the derived projected surface density distribution shown in figure 6. Figure 5 shows the array of line profiles altered by the above procedure. Some things should be noted in the figure. The profile at $l^{II} = 22°.0$, $b^{II} = -3°.0$ has a velocity significantly less than the main section of the cloud. Shane's observations indicate that this lower velocity feature can be traced back to the galactic equator. Secondly, the peripheral profiles generally show a two-humped structure; the scale of this structure is close to the sensitivity of the measurements, but the general recurrence of the structure indicates that it is real. Thirdly the profiles generally are somewhat flatter on the low velocity sides of the peaks. The simplest explanation for all these facts is that the radiation of the feature is superimposed upon a weak, slightly lower-velocity source that is part of the galactic structure. This hypothesis was tested further by reducing the profile for $l^{II} = 20°$, $b^{II} = -4°$ again, this time allowing for the presumed galactic source. The result is shown by the dotted profile in figure 5; it agrees more with the other profiles than did the original altered profile. No further attempts were made to correct the other profiles, both because of the lack of information and because of the relatively small size of the contribution.

Data calculated from the profiles are presented in table 1. Several profiles showing traces of the feature are not included because of the impossibility of making reliable estimates. The table contains the following information:

1) Galactic longitude l^{II}.
2) Galactic latitude b^{II}.

TABLE 1

Observations

l^{II}	b^{II}	T_b(max) (°K)	V_{CM} (km/sec)	σ (km/sec)	V_r (km/sec)	$N_H \times 10^{-19}$ (atoms/cm²)
21°.0	− 4°.0	1.0	117.7	7.3	+ 1.9	3.4
21.0	− 5.0	1.4	117.6	9.0	+ 1.8	6.0
21.5	− 3.5	3.6	115.0	7.6	− 0.8	12.9
21.5	− 4.5	4.3	117.1	9.9	+ 1.3	18.1
22.0	− 4.0	4.7	114.6	10.1	− 1.2	18.6
22.0	− 5.0	2.4	115.5	7.8	− 0.3	8.8
22.5	− 3.5	3.2	113.8	6.2	− 2.0	9.1
22.5	− 4.5	2.6	115.6	6.8	− 0.2	8.0
22.5	− 5.5	1.2	116.8	7.6	+ 1.0	3.8
23.0	− 3.0	0.8	116	—	+ 0.2	1.3
23.0	− 4.0	1.5	117.1	8.8	+ 1.3	6.0

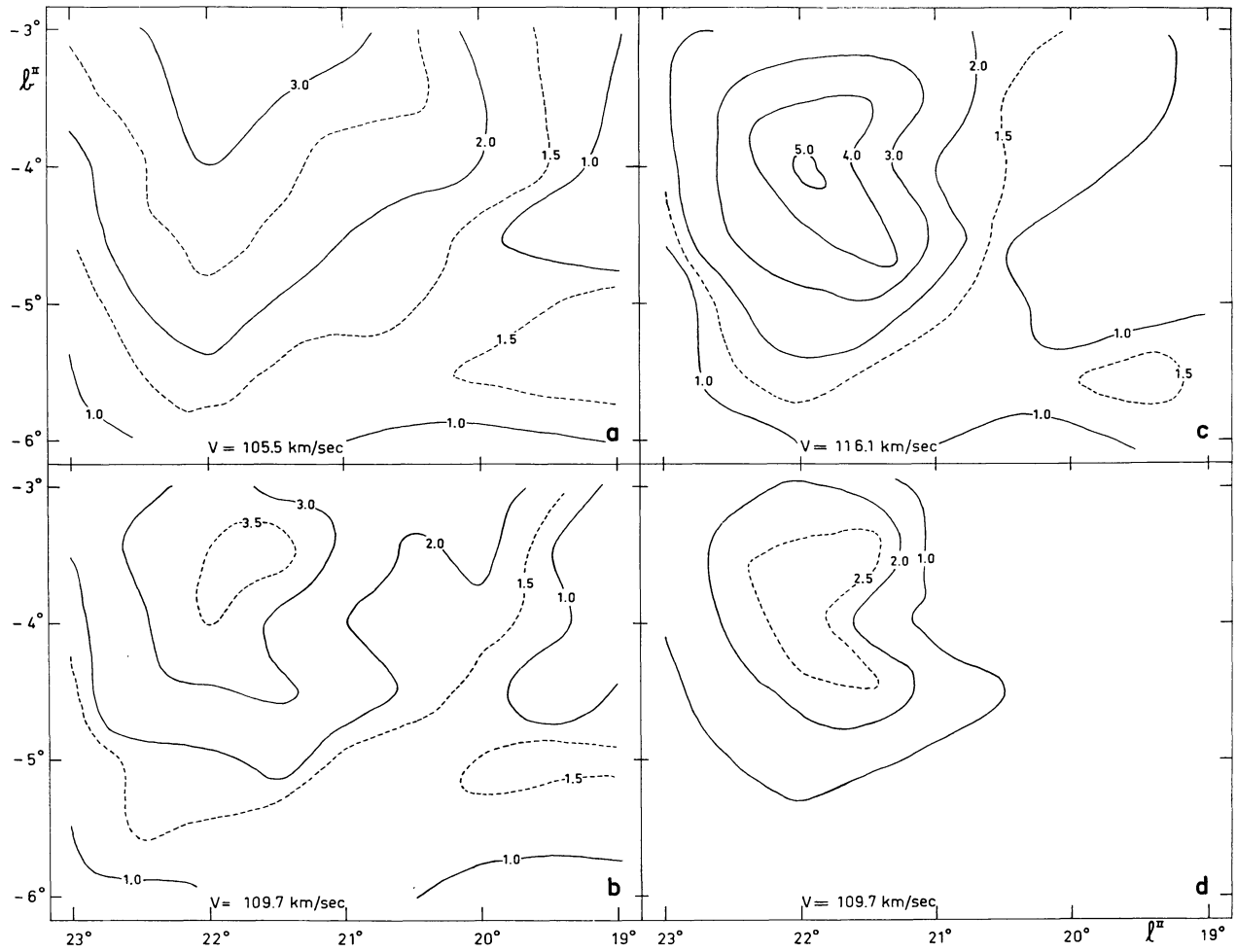

Figure 4. Contour maps of brightness temperature at constant velocity constructed from the observed profiles (figures 4a, b, c) and from the profiles after subtraction of the extrapolated galactic structure (figure 4d).

3) The maximum brightness temperature $T_b(\max)$ for the altered profile, where T_b is defined by the Rayleigh-Jeans law for intensity

$$I = (2v^2/c^2)kT_b .$$

4) The centre of mass velocity for the column along the line of sight

$$V_{CM} = \Sigma_i T_{bi} V_i / \Sigma_i T_{bi} .$$

The V_i are separated by 2.11 km/sec.

5) The dispersion in velocity

$$\sigma = \sqrt{(\Sigma_i T_{bi}(V_{CM} - V_i)^2 / \Sigma_i T_{bi})} .$$

Values for the weak profiles are low because of the restricted velocity range over which the summation could be executed.

6) The residual velocities V_r as measured from the centre of mass velocity for the entire cloud, 115.8 km/sec.

7) The total number of neutral hydrogen atoms per cm^2 along the line of sight. The relation between neutral hydrogen content and integrated optical depth is

$$N_H = 1.835 \times 10^{13} T \int \tau(V) dV ,$$

where T is the gas temperature, τ is the optical depth and dV is expressed in cm/sec (VAN DE HULST, MULLER and OORT, 1954).

For small optical depths the equation

$$\frac{T_b}{T} = \frac{I}{I_0} = 1 - e^{-\tau}$$

becomes $\tau = T_b/T$. Using this fact and expressing V in

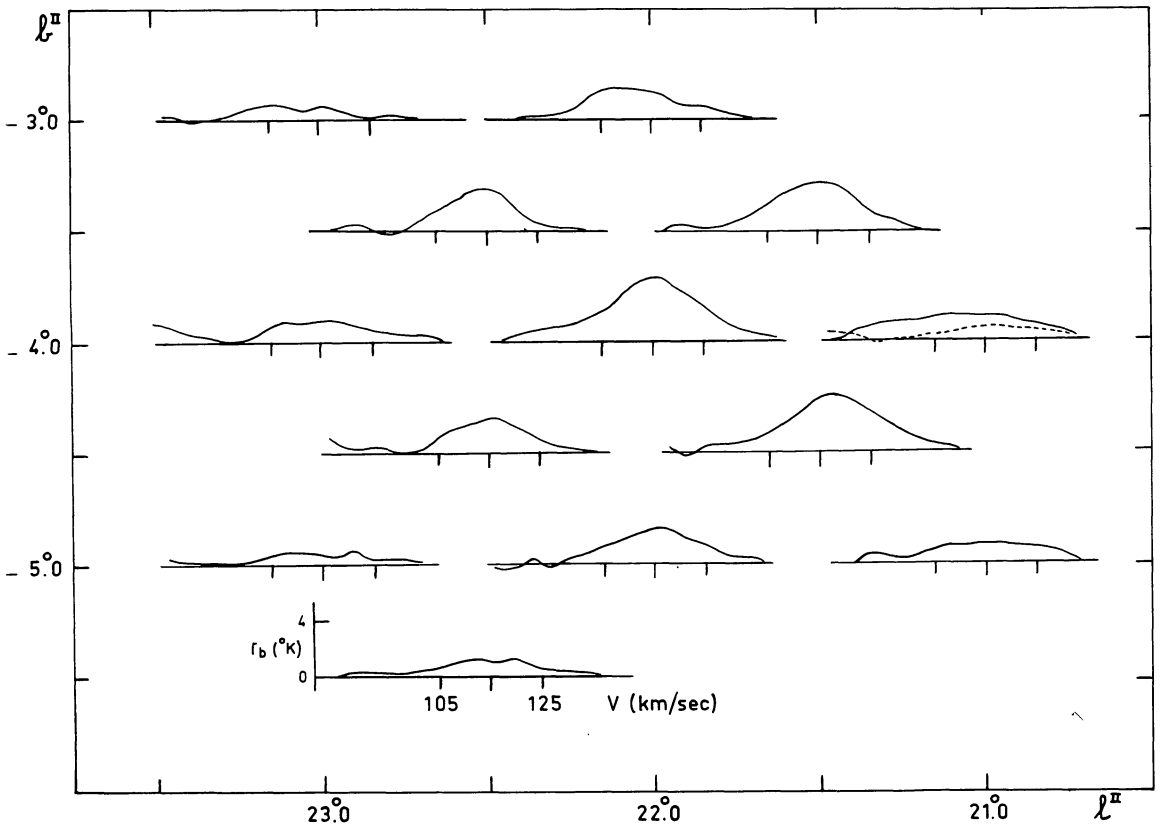

Figure 5. All profiles showing the feature, after subtraction of the extrapolated galactic structure. The velocity scale is the same for all profiles. The profiles are arranged according to their positions in the sky. The significance of the dashed profile is explained in the text.

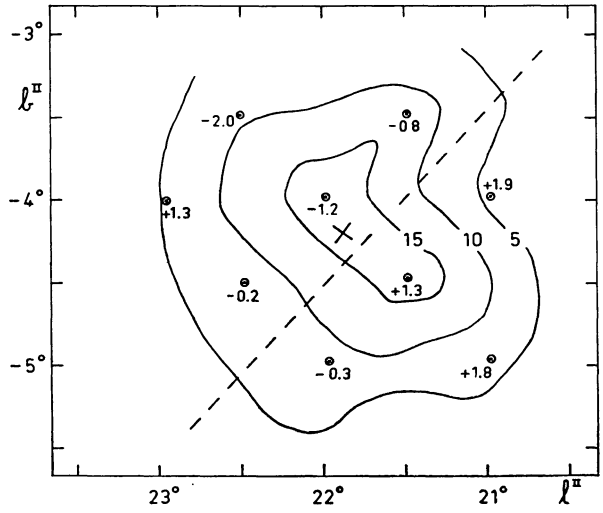

Figure 6. Contour map of the number of neutral hydrogen atoms per cm² within the feature, integrated along the line of sight. The contour units are 10^{19} atoms/cm². The figure also shows the position of the centre of mass (×), the mean velocities with respect to the centre of mass at several points (○) and the direction of the proposed axis of rotation (broken line).

km/sec we obtain

$$N_H = 1.835 \times 10^{18} \int T_b \, dV,$$

and it is no longer necessary to assume a gas temperature for the feature unless the temperature is exceedingly low. For the actual evaluation the integral was replaced by $\Sigma_i T_{bi} \Delta V$.

Figure 6 is a contour map of projected surface densities based on column 7 of table 1. The contour values are in units of 10^{19} atoms/cm²; the small numbers

TABLE 2

Parameters as a function of distance

R (kpc)	M_H (solar masses)	r_0 (pc)	$\overline{N_H}$ (atoms/cm³)	$\overline{N_H}$ (max) (atoms/cm³)
0.2	47	5.2	3.2	11.5
1.0	1200	26	0.63	2.3
9.3	1.0×10^5	240	0.07	0.25
240	6.8×10^7	6300	0.003	0.01
1200	1.7×10^9	34000	0.0005	0.002

represent the residual velocities, and the × locates the centre of mass, $l^{II} = 21°.9$, $b^{II} = -4°.2$.

The total atomic hydrogen mass of the feature is 1200 R^2 solar masses, where R is the distance in kiloparsecs. The centre of mass velocity with respect to the local standard of rest is 115.8 km/sec, and the velocity dispersion of the cloud is 8.6 km/sec. The angular diameter is about 3°. Table 2 gives, for several possible distances, the mass M_H, the size r_0, the mean hydrogen density $\overline{N}_H$ assuming the dimension along the line of sight is the same as the transverse dimensions, and the mean hydrogen density $\overline{N}_H(\max)$ in the direction of the most intense radiation, making the same assumption.

A study of the Palomar Sky Survey revealed nothing peculiar in the region of the feature. The absorption grows heavier to the equatorial south, and there are some absorption lanes running north-east to another area of heavier absorption. Many stars are visible, indicating that there is not much local absorption.

2. Interpretation

Various possible interpretations of the feature are:

1) That it is an extra-galactic object
2) That it is a deviant fragment of galactic structure
3) That it is a part or the whole of a supernova shell or
4) That it is simply a high velocity cloud.

The high velocity of the feature with respect to the local standard of rest and information concerning its physical parameters should be kept in mind when the likelihood of each possibility is considered.

The virial theorem limits the range of possibilities, and it is helpful to develop estimates of the various terms before further discussing the above alternatives; the terms will be functions of the distance R. The scalar form is (WOLTJER)

$$\frac{1}{2}\frac{d^2I}{dt^2} = 2T + 3U + W + M + \frac{1}{4\pi}\int_S (\boldsymbol{r}\cdot\boldsymbol{B})\boldsymbol{B}\cdot d\boldsymbol{S} - \int_S \left(P + \frac{B^2}{8\pi}\right)\boldsymbol{r}\cdot d\boldsymbol{S},$$

where $T = \frac{1}{2}\int u^2\, dm$, $U = \int P\, dV$, $M = \int (B^2/8\pi)\, dV$, $I = \int r^2\, dm$, $W = \int \boldsymbol{r}\cdot\nabla\Phi\, dm$, u = mean velocity of a mass element, dm = element of mass, Φ = gravitational potential, $\boldsymbol{B}$ = magnetic field, dV = volume element, and P = pressure. Since the observations do not make the conceptual distinction between motion of elements and motion within elements it is convenient to combine twice the translational energy from thermal motions, which turns out to be $3U$, with the $2T$ defined above into one term $2T'$.

The kinetic energy term is the most easily determined. The kinetic energy of a column of gas is $\frac{1}{2}M_i(\sigma_i^2 + V_{ri}^2)$, where M_i is the mass of the column, σ_i the dispersion, and V_{ri} the residual velocity. Thus for each observed point the kinetic energy separates into two components, one due to the random motions within the column and one due to the net motion of the column with respect to the centre of mass of the system. Summing the random motion components and multiplying by three to account for motion in the transverse directions leads to a contribution to $2T'$ of $5.1 \times 10^{48} R^2$ erg/kpc². The component relating to the residual velocities is more complicated, for the observed residual motions can reflect four things, of which only two give real contributions to the kinetic energy. The first possible explanation of the residual velocities is that they are caused by random macroscopic motions within the cloud. In this case one proceeds as above, summing and multiplying by three; this gives a net contribution of $2(3\Sigma_i \frac{1}{2}M_i V_{ri}^2) = 1.1 \times 10^{47} R^2$ erg/kpc². The regularity of the residual motions in the central parts of the cloud, however, suggests rotation about an axis whose projection is represented by the broken line in figure 6. For pure rotation the contribution is $(7.2 \times 10^{46} R^2/\sin^2 i)$ erg/kpc², where i is the angle between the axis and the line of sight. Thirdly, the variance of the angle between the line of sight and the line of motion for observations in different directions results in apparent motion with respect to the centre of mass, given approximately by $\Delta V = \alpha V_0 \operatorname{tg} \beta$ where α and β are the angles indicated in figure 7. An angle of $\beta = 30°$ would give $\Delta V = 1.2$ km/sec·degree across the feature. The nonlinearity of the actual residual velocities indicates that this effect at most modifies one of the first two explanations. Also, the most probable explanation of the feature as a detached part of the galactic structure near the closest point to the galactic centre implies a small β. Finally, the residuals could reflect systematic and random errors in the subtraction process; random errors are especially likely for the weak profiles, and systematic errors between strong and weak profiles can be expected.

In any case, the second contribution to the kinetic energy is much less than the first unless rotation with a small inclination to the line of sight exists. If no aligning forces are present, the probability that the rotation term reaches a value greater than one half the first term is less than one per cent. A value of $5.2 \times 10^{48} R^2$ erg/kpc^2 was adopted for the kinetic term for the neutral hydrogen.

Both self-gravitation and galactic gravitation contribute to W; the second contribution is important only

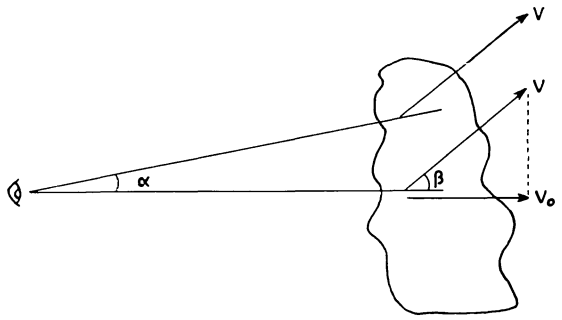

Figure 7. Variations in observed velocity across the feature due to transverse motion. V is the space velocity and V_0 the radial velocity. The figure illustrates the angles α and β referred to in the text.

near the galactic centre. The self-gravitational term was estimated in two ways. First, the observed density distribution was fitted roughly to a power law of the form $\rho \propto r^{\alpha}$. The integral defining W was evaluated for a model following the power law, and a value of $-4.5 \times 10^{45} R^3$ erg/kpc^3 was found. Secondly, the integral was replaced by a sum representing the self-gravitation of elements at each observation point and the gravitational interactions of these elements. This led to an estimate of $-4.1 \times 10^{45} R^3$ erg/kpc^3. Thus a reasonable estimate would seem to be $-4.3 \times 10^{45} R^3$ erg/kpc^3 for the neutral hydrogen. SCHMIDT's (1956) model of the galactic gravitational field was used to estimate the galactic contribution. For $R = R_m = 9.3$ kpc, the distance at which the line of sight comes closest to the galactic centre, a value of $+5.3 \times 10^{46} R_m^3$ erg/kpc^3 was found; the sign of the term is such as to be disruptive. The term is less important at other distances.

Not much can be said about the volume and surface magnetic terms. If a sphere of radius r_0 is taken that encloses the cloud, and if the magnetic field makes no preferred angle with the surface of the sphere, the magnetic terms reduce to

$$\tfrac{1}{6} r_0^3 (\langle B^2 \rangle_V - \langle B^2 \rangle_S) \text{ erg},$$

where terms in angular brackets denote averages over the volume and the surface respectively. If a radius of 1°.5 is taken and if B is expressed in microgauss, the net magnetic term becomes $8.6 \times 10^{46} \Delta \langle B^2 \rangle R^3$ erg/kpc^3, where the Δ indicates the difference between the volume and surface averages. Thus a difference between the root mean square values of B of 0.2 μG would make the magnetic terms comparable to the neutral hydrogen self-gravitation term; both vary with R^3. The difference between the central and boundary values for B can be appreciably greater than the difference between the surface and the volume averages.

Now, using the estimates developed above, we may look more closely at the various possible interpretations of the feature.

1) *Extra-galactic object.* If the feature is extra-galactic it is reasonable to assume it is an isolated object in equilibrium. Let the total mass be qM_H. If the total mass is distributed in space and in velocity in a manner similar to the hydrogen mass, then $T' = qT'_H$ and $W = q^2 W_H$. For a magnetic field decreasing from 1 μG at the centre to 0 at the boundary and for a q of 5, the net magnetic term is small enough to be dropped from the virial theorem. The remaining terms and assumptions yield a distance of $(1200/q)$ kpc. This distance, in turn, gives a total mass of $(1.7 \times 10^9/q)$ solar masses and a radius of $(31/q)$ kpc.

Table 3 lists a few representative quantities for the Magellanic Clouds, for two dwarf galaxies, and for the feature. A value of 10 was used for q, corresponding to the Magellanic Clouds. The feature bears no particular resemblance to known extra-galactic objects; furthermore, its projected velocity with respect to the centre of the galaxy is 210 km/sec, which is greater than the velocity of escape from the Local Group. Although none of these considerations rule out an extra-galactic interpretation, they do nothing to support it.

2) *Detached segment of galactic structure.* The maximum velocity observed for the neutral hydrogen component of galactic structure at the galactic longitude of the feature is within 10 km/sec of the velocity of the feature itself (see figure 2). It would seem possible that

TABLE 3

Comparison with extragalactic objects

	LMC†	SMC†	Fornax*	Sculptor**	feature ($q = 10$)
R (kpc)	46	46	188	83	120
M_H (solar masses)	5.5×10^8	4.5×10^8	—	—	3.4×10^7
M_T (solar masses)	8×10^9	1.3×10^{9}††	2×10^7	3×10^6	1.7×10^8
r_0 (kpc)	5	13	3.3	1.1	3.1
σ (km/sec)	20††	—	—	—	8.6

† J. V. HINDMAN, F. J. KERR and R. X. MCGEE, 1963, *Austr. J. Phys.* **16** 570. For comparison's sake the hydrogen in the bridge was apportioned between the LMC and SMC.

†† F. J. KERR and G. DE VAUCOULEURS, 1956, *Austr. J. Phys.* **9** 90

* P. W. HODGE, 1961, *A.J.* **66** 249

** P. W. HODGE, 1961, *A.J.* **66** 284

the feature is a detached portion of the galactic structure. The morphological fit is strengthened by the fact that the velocity dispersion in the feature agrees fairly well with the dispersions in the adjoining galactic structure. The near agreement of the velocity of the feature with the maximum velocity observed in the galactic plane at the same longitude suggests that the feature should be located along the line of sight near the point where it most closely approaches the galactic centre, at a distance of 9.3 kpc from the Sun. At this location the feature cannot be in equilibrium without a confining magnetic field having $(-\Delta\langle B^2\rangle)^{\frac{1}{2}} = 3\mu$G in the case of pure atomic hydrogen or $(-\Delta\langle B^2\rangle)^{\frac{1}{2}} = 4\mu$G for the case where the feature is 50 per cent atomic hydrogen by mass. However, equilibrium need not be expected. The time dependent term of the virial theorem permits an estimate of a characteristic time for which the feature will double in size. For $(\Delta\langle B^2\rangle)^{\frac{1}{2}} = 0$ this time is 5×10^6 years; for $(+\Delta\langle B^2\rangle)^{\frac{1}{2}} = 3$ to 4 μG the time is about 4×10^6 years. Even in the case where a disruptive magnetic field is the dominant effect, say $(+\Delta\langle B^2\rangle)^{\frac{1}{2}} = 10\,\mu$G the characteristic expansion time is more than 10^6 years. Thus, although the feature probably is not in equilibrium, the degree of inequilibrium is small enough to keep the theory attractive.

3) *Supernova shell.* If the feature is a whole supernova shell, then we must assume that the mean radial velocity is 115.8 km/sec and that the shell expansion velocity has fallen to values comparable to the random motions in the shell, thus giving a single-humped profile. For the feature, the velocity of expansion would probably be no greater than 5 km/sec. The supernova is assumed to be Type II, since the ejection of Type I is too small to account for the total mass. The drawback to this hypothesis is its inability to explain the high velocity of the supernova with respect to the local standard of rest. If one assumes that the supernova had an initial expansion momentum of 7.5×10^3 solar masses·km/sec (MINKOWSKI, 1959) and uses the fact that the current mass and hence momentum is a function of distance, conservation of momentum implies a distance of 1.2 kpc. Type II supernovae generally are Population I stars for which such a high relative velocity is not expected at this distance. In addition, the observed density distribution is not what one would expect from a complete shell.

The fragmentary shell hypothesis is somewhat more attractive for it explains the high velocity by attributing it to the shell expansion velocity. If the space velocity of the fragment made an angle with the line of sight greater than 45°, the projection effect mentioned earlier would become greater than 2 km/sec·degree and would be noticeable. Thus the angle is probably less than 45° and the true velocity less than 165 km/sec. If we take 116 km/sec as the present expansion velocity and suppose that the fragment received one part in k of the original momentum, the same considerations used for the complete shell give a distance of $(250/k)$ pc. This value is directly proportional to the square root of the present velocity. If the fragment were decelerated solely by sweeping through an interstellar medium of $n = 0.1$ atoms/cm^3, it would take 40 000 years to slow to 116 km/sec. If $n = 1.0$ the figure becomes 20 000 years. In both cases the age is less than the

100 000 years one gets as a characteristic disruption time for the fragment from the virial theorem. The comparative newness and closeness of the fragment derived from these considerations conflict with the absence of an optical object, especially since local obscuration in the direction of the feature seems small.

4) *High-velocity cloud.* The high velocity with respect to the surrounding medium argues against this interpretation. If a diameter of 10 pc is assumed, the cloud would lie 200 pc away and 15 pc below the galactic plane. The average density of the cloud at this distance, 3 hydrogen atoms per cm^3, is not much greater than the mean density of the interstellar medium, and it is difficult to see how such a relatively diffuse cloud could remain coherent while moving at more than 100 km/sec through the interstellar medium. On the other hand, except for its low latitude, the feature closely resembles the clouds studied by MULLER, OORT and RAIMOND (1963).

These considerations and particularly the close apparent association of the feature with the structure in the galactic plane seem to suggest that the feature may be a fragment dissociating from the main body of galactic structure. It bears a close similarity to the feature discussed by Mrs Bieger-Smith (SMITH, 1963); this latter feature, however, is five times larger than the one discussed here, and it is less intimately connected with the galactic structure.

Acknowledgements

I would like to acknowledge a Fullbright grant and to thank the United States Educational Foundation in the Netherlands for their support. I am grateful for the hospitality extended to me by Professor Oort and the Leiden Observatory. In particular, I wish to thank W. Shane for suggesting this work, for providing the observations, and for his continued helpful interest.

References

H. C. VAN DE HULST, C. A. MULLER and J. H. OORT, 1954, *B.A.N.* **12** 117 (No. 452)
R. MINKOWSKI, 1959, *Paris Symposium on Radio Astronomy* (*I.A.U. Symp.* No. 9) 315
C. A. MULLER, J. H. OORT and E. RAIMOND, 1963, *C.R.* **257** 1661
E. RAIMOND, 1962/63, *Sitzber. Akad. Heidelberg* **2** 123
M. SCHMIDT, 1956, *B.A.N.* **13** 15 (No. 468)
G. P. SMITH, 1963, *B.A.N.* **17** 203
L. WOLTJER, *Stars and Stellar Systems* **5** (in press)